International Journal of Microwave and Wireless Technologies, 2011, 3(6), 621–625.
doi:10.1017/S1759078711000663

RESEARCH PAPER

High-efficiency inverse class-F power amplifier using 3/4 spiral symmetric defected ground structure

SHILEI JIN, JIANYI ZHOU AND LEI ZHANG

In this article, the development of a high-efficiency power amplifier (PA) with the inverse class-F configuration and a novel 3/4 spiral defected ground structure (DGS) is presented. The proposed DGS structure has improved rejection characteristic and its resonance frequencies are more convenient to adjust than conventional symmetric and asymmetric spiral structure. The electromagnetic-simulated result shows that the proposed circuit has improved harmonic control performance with simplified structure and less return loss than the conventional microstrip harmonic control circuit. The 3/4 spiral harmonics control circuit (HCC) can be modeled by three parallel RLC resonators. Using the proposed structure a high-performance harmonic control circuit is designed for implementing an inverse class-F PA. For comparison, two inverse class-F PAs operating at 2.4 GHz have been implemented by the microstrip HCC and the proposed HCC, respectively. According to the experiment results, the size of the proposed inverse class-F PA is reduced by 20%, the power-added efficiency and the gain are increased by 4.8% and 1.5 dB, respectively.

Keywords: 3/4 Spiral defected ground structure (DGS), Harmonic control circuit (HCC), Inverse class-F PA, Power-added efficiency (PAE)

Received 8 February 2011; Revised 10 May 2011; first published online 1 July 2011

I. INTRODUCTION

The power amplifier (PA) is one of the most significant components in a RF transceiver system. With the growing interest in developing modern wireless communication systems, such as wideband code division, wireless local area network, and worldwide interoperability for microwave access, more PAs with high efficiency are needed [1]. In order to increase the efficiency of PAs many technologies have been proposed such as class-E PAs, class-F PAs, and Doherty PAs [2–4]. Among these technologies the class-F PA, which has short load termination at even-order harmonics and open load termination at odd-order harmonics, can achieve high efficiency with the advantages of high operational frequency and small size. Recently, there has been more focus on the inverse class-F amplifiers, which have open load termination at even-order harmonics and short load termination at odd-order harmonics. The inverse class-F PAs can deliver higher efficiency than class-F amplifiers with the similar technology [5–7].

The defected ground structure (DGS) has shown increasing potential in several applications [8–13]. The microstrip with DGS implemented by making artificial apertures on the ground plane can provide resonance property and the resonance frequencies vary depending on the size of the structure. DGS also provides additional effective inductance which can provide longer electrical length than conventional microstrip. Many types of DGSs have been presented, such as dumbbell DGS, spiral DGS, and tapered DGS [14–16]. Among these different structures the spiral shape structure has become the most potential one due to its characteristic of multi-rejection band. The microstrips with spiral DGSs of different configurations have been reported such as the symmetric and asymmetric spiral DGS [14, 17]. However the resonance frequencies of conventional structures are difficult to control.

Harmonics control circuit (HCC) is the key part of inverse class-F PAs. Conventionally, there are two methods to design HCCs: lumped method and microstrip method. Due to the low-*Q* value of inductances, the performance of inverse class-F amplifiers implemented by lumped HCCs is limited. Additionally, the microstrip HCC will increase the size of PAs and is difficult to include more harmonics than three orders.

In this article a high-performance HCC with single symmetric 3/4 spiral DGS was proposed to implement inverse class-F PAs. Compared with conventional spiral DGSs, the 3/4 spiral DGS has similar performance but smaller size and improved controllability. The proposed HCC can achieve a simplified structure and improved performance by inserting the proposed 3/4 spiral DGS. Additionally, the transistor drain–source capacitance which limits the efficiency in conventional inverse class-F PAs can be ignored due to the rejection characteristic provided by the proposed 3/4 spiral DGS. For comparison and validation, two inverse class-F PAs with

Department of Radio Engineering, School of Information Science and Engineering, Southeast University, Liwenzheng Lou, North Room 633, Nanjing 210096, China
Corresponding author:
S. Jin
Email: jinshilei@gmail.com

the proposed HCC and conventional HCC have been implemented. The experimental results show that the performance of the proposed inverse class-F PA is enhanced with reduced size contrast to the conventional inverse class-F PA.

II. 3/4 SPIRAL DGS

The schematic diagram of a microstrip with the proposed DGS unit is depicted in Fig. 1. The line width of the microstrip is chosen for the characteristic impedance of 50 Ω. The thickness and the dielectric constant of the applied substrate are 0.5 mm and 2.65, respectively. The dimensions of the structure are labeled in Fig. 1. The value of F is three times that of E and the value of G is determined by the number of spiral turns.

Compared with conventional spiral DGSs the proposed DGS is easy to control the resonance frequencies. When E, F, and G are constant, the resonance frequencies vary depending on the values of A, B, C, D, and H. If the five variables are all increased by the same values (the spiral structure is fixed symmetric), the two resonance frequencies decrease and the changing velocity of the second one is twice of the first one. However when the five variables are changed, respectively, the changing velocities of the resonance frequencies are different. The simulation results of transfer characteristics are illustrated in Fig. 2 where H is changed individually and all the five variables are reduced simultaneously.

In practical when the DGS is employed to design microwave components, especially RF PAs, a metal stub should be applied to dissipate heat. Therefore there must be a cavity located below the DGS in the metal stub as shown in Fig. 1. Since the DGS utilizes the defects on the ground plane, it is necessary to examine the effects of the size of the cavity to the proposed DGS. The simulated transfer characteristics against different sizes of the cavity are shown in Fig. 3. The height of the metal stub is fixed to 3 cm. If the cross-section area of the cavity is smaller than the DGS's size, radiation will be affected seriously. The effects can be ignored when the area is larger than 3 cm^2. However the cavity reduces the heat sinking ability of the metal stub which may cause damage to components. For this reason a tradeoff should be achieved if the DGS is used to design high-power devices.

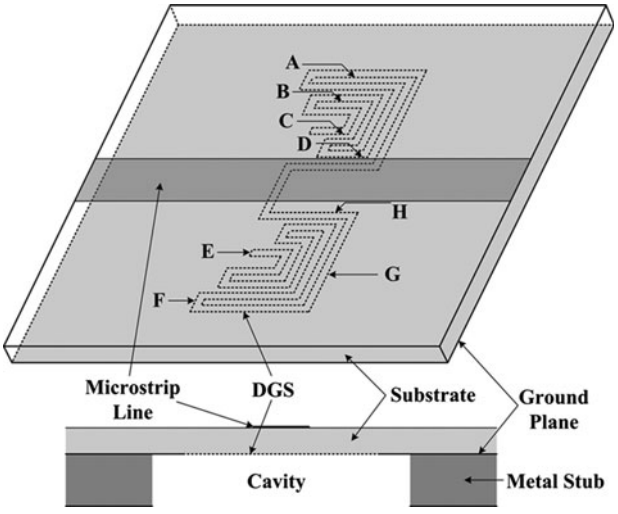

Fig. 1. Microstrip with the proposed 3/4 spiral DGS.

III. HARMONICS CONTROL CIRCUIT

The drain voltage waveform of an inverse class-F amplifier includes one or more even harmonics and approximates a half sine wave, whereas the current waveform includes odd harmonics and approximates a square wave. In theory, the efficiency increases as more harmonics are included, approaching the ideal efficiency of 100% for the case when all the harmonics are included [5]. However, including more harmonics increases the complexity of a HCC and gives rise to insertion loss. An inverse class-F PA can achieve the drain efficiency higher than 80% if the second, third, and fourth harmonics are included.

A) Structure of 3/4 spiral DGS HCC and conventional HCC

The proposed HCC is designed to provide the control of up to the fourth harmonic. For comparison a conventional microstrip HCC has been implemented. Figure 4 is depicted as the block diagrams of the conventional HCC and 3/4 spiral DGS HCC. The dimensions of the 3/4 spiral DGS applied in the HCC are $A = 2.6$, $B = 1.4$, $C = 1.2$, $D = 1$, $E = 0.2$, $F = 0.6$, $G = 3.2$, and $H = 2.6$ (the unit is millimeter). Both of the harmonic control circuits are designed with consideration of parasitic-output capacitance C_{out} which is drain–source capacitance plus gate–drain capacitance of FET device. To compensate for C_{out} in the proposed HCC, the electrical length θ_1 of DGS microstrip was slightly modified to provide an open-circuit condition for the second and fourth harmonics and the electrical length θ_2 of the microstrip between DGS and $\lambda/12$ shunt microstrip was properly modified to provide a short-circuit condition for the third harmonic.

B) Characteristics of the two HCCs

Figure 5 is shown as the measured frequency characteristics and calculated impedance characteristics of the two HCCs where C_{out} is included. The frequency responses show that both of the HCCs can provide three stopbands: 4.8, 7.2, and 9.6 GHz and the fundamental signal (2.4 GHz) can pass

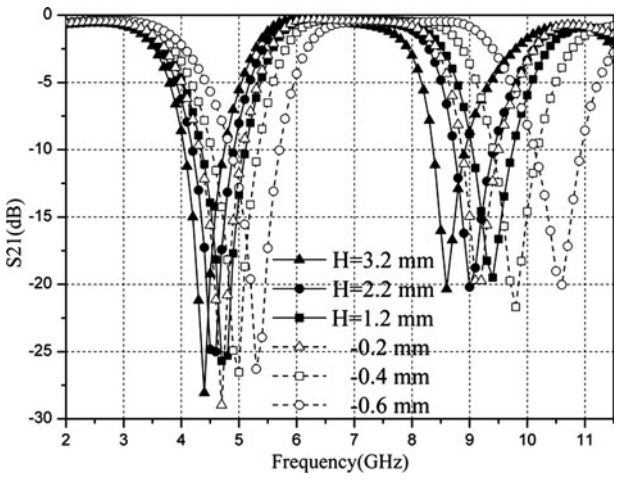

Fig. 2. Simulated transfer characteristics of the proposed DGS with different dimensions.

https://doi.org/10.1017/S1759078711000663 Published online by Cambridge University Press

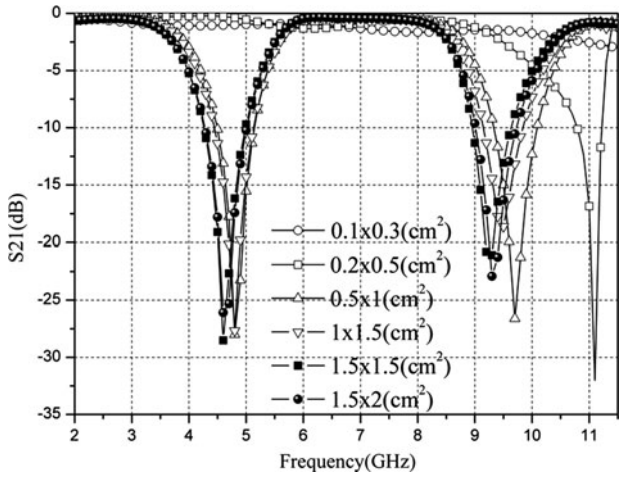

Fig. 3. Simulated transfer characteristics of the proposed DGS against different sizes of the cavity.

without attenuation. The first and third stopbands of the proposed HCC are the resonance frequencies of the DGS, the second stopband is due to the $\lambda/12$ stub. The first and third stopbands of the conventional HCC are caused by the $\lambda/4$ microstrip and the second stopband is due to the $\lambda/12$ stub. The second harmonic loads of the two circuits are higher than 700 Ω and the third harmonic load is lower than 2.5 Ω. However the forth harmonic load of the proposed HCC and conventional HCC are 440 and 2 Ω, respectively. Accordingly, we can draw the conclusion that the proposed HCC can include the forth harmonic. As the conventional HCC is concerned, providing both the second and fourth harmonic open-circuit terminations simultaneously is complicated and increases the insertion loss.

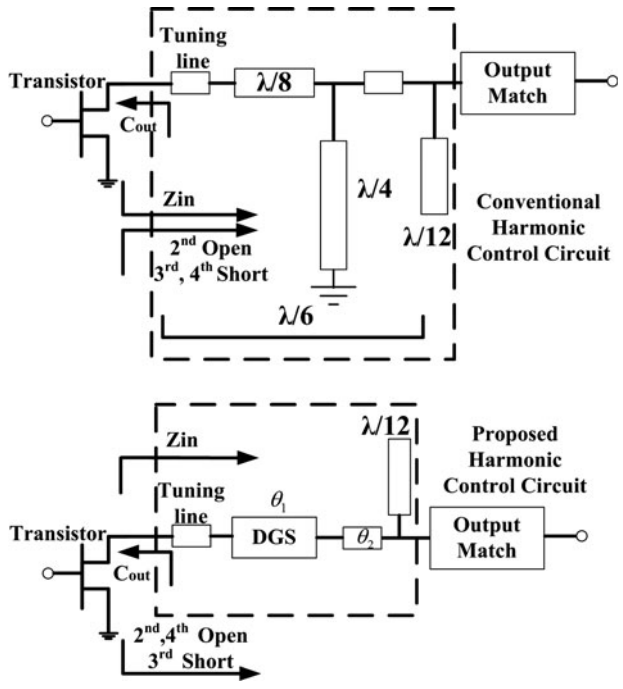

Fig. 4. Block diagrams of conventional harmonic control circuit and the proposed harmonic control circuit.

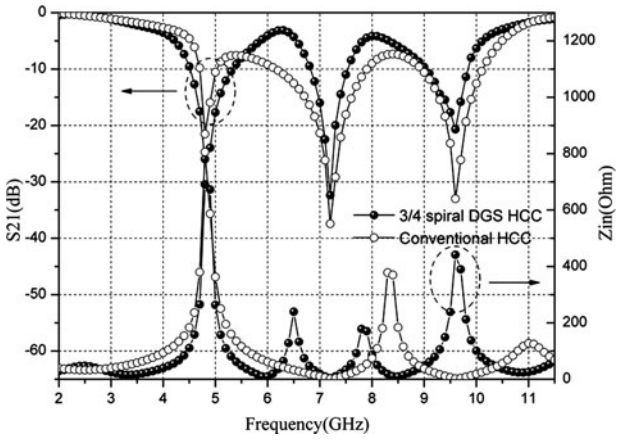

Fig. 5. Measured frequency characteristics and calculated impedance characteristics of the two HCCs.

C) Equivalent circuit of the 3/4 spiral DGS HCC

The 3/4 spiral DGS HCC can be modeled by three parallel RLC resonators (shown in Fig. 6). The resonance frequencies of the resonators connected in series are 4.8 and 9.6 GHz and the parallel resonator resonates at 2.4 GHz. The circuit parameters of the equivalent circuit can be extracted by (1), (2), and (3) according to the simulation results of *S*-parameter shown in Fig. 5 [18]. In these equations ω_n and ω_{cn} denote the resonance angular frequencies and 3-dB cutoff angular frequencies, respectively, and Z_o is the characteristic impedance of the microstrip. The calculated results are shown in Fig. 6.

$$C_n = \frac{\omega_n}{2Z_o(\omega_n^2 - \omega_{cn}^2)}, \tag{1}$$

$$L_n = \frac{1}{4\pi^2 f_n^2 C_n}, \tag{2}$$

$$R_n = \frac{2Z_o}{\sqrt{(1/|S_{11}(\omega_n)|^2) - (2Z_o(\omega_n C_n - (1/\omega_n L_n)))^2} - 1} = \frac{2Z_o}{(1/|S_{11}(\omega_n)|) - 1}, \quad n = 1, 2, 3 \tag{3}$$

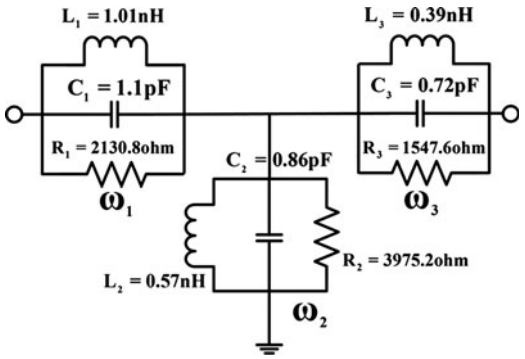

Fig. 6. Equivalent circuit of the 3/4 spiral DGS HCC.

https://doi.org/10.1017/S1759078711000663 Published online by Cambridge University Press

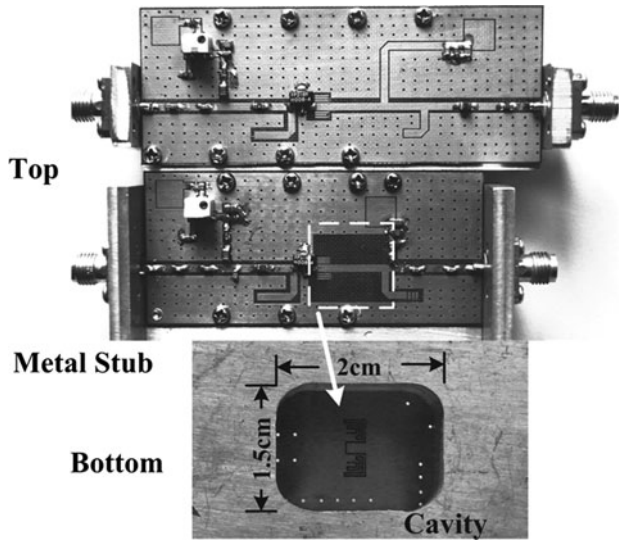

Fig. 7. Photo of the inverse class-F PAs.

D) Conclusion

Compared to the conventional microstrip HCC, the 3/4 spiral DGS HCC including the second, third, and fourth harmonic can enhance the performance of inverse class-F PAs effectively. Adoption of the DGS increases the effective series inductance of the microstrip which can provide longer electrical length than the conventional microstrip. Therefore the proposed HCC is simplified and its size is reduced.

IV. INVERSE CLASS-F PA

A) Input matching network

The input voltage of RF transistors has a severe nonlinear distortion due to the gate–source capacitance C_{gs} which is the main cause of signal distortion at the gate terminal, especially when the bias is set around the pinch-off voltage [19]. The distortion destroys the idealized sinusoidal excitation which decreases the efficiency of PAs. In the input matching circuit of the proposed PA, a parallel $\lambda/8$ stub at the gate of the transistor is applied as short-circuit input harmonics to eliminate the influence of input distortion.

B) Bias voltage setting

The transistor employed to implement the inverse class-F PA is a low-cost 1-W heterostructure FET. The optimal drain bias voltage of the transistor is 8 V and the breakdown voltage is 16 V. Since the high peak drain voltage of inverse class-F PAs, measurement must be done at a lower drain bias to avoid voltage breakdown. When the voltage is above 7 V the amplifier is unstable. However the performance of the PA will degrade due to the low drain voltage. Therefore the bias voltage is set as 5.5 V to achieve a tradeoff between the output power and the drain efficiency without any possibility of voltage breakdown.

C) Comparison results of two inverse class-F PAs

To show the advantage of the proposed inverse class-F PA, an inverse class-F PA was presented implemented by the conventional HCC at the condition of the same transistor, input matching network, and bias voltage. Figure 7 is the photo of the two PAs in which we can see the cavity in the metal stub. The dimension of the cavity is 1.5 cm × 2 cm. The size of the proposed PA is reduced from 3 cm × 7.8 cm to 3 cm × 6.3 cm.

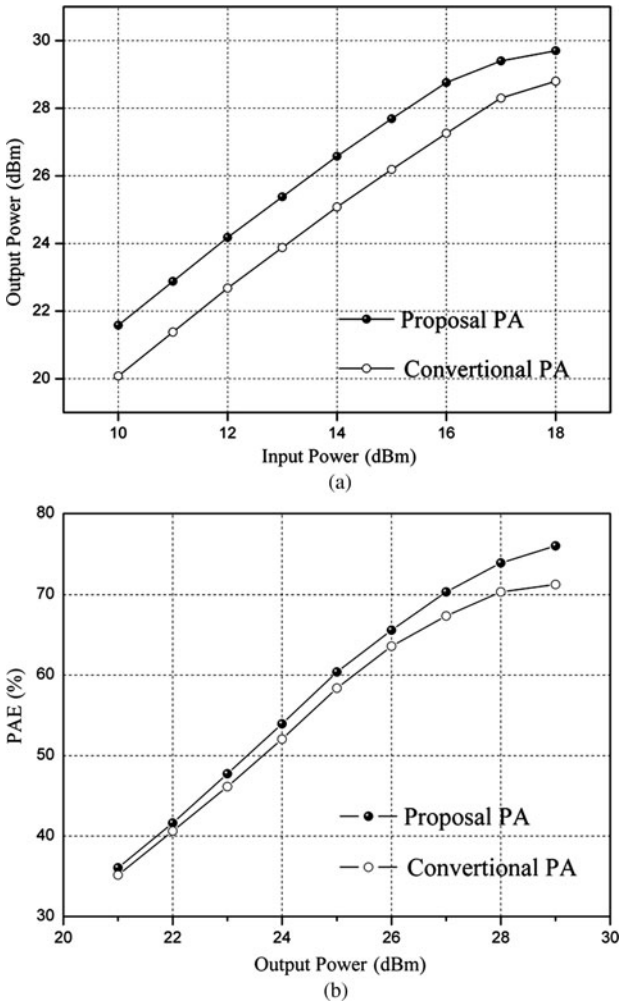

Fig. 8. (a) Output power performance of the two PAs. (b) PAE performance of the two PAs.

The measured output power performance of the two PAs is shown in Fig. 8(a). The gain of the proposed inverse class-F PA is improved by 1.5 dB due to lower loss of the 3/4 spiral HCC than the conventional HCC. Figure 8(b) is illustrated as the PAE results of the two PAs in which we can see that the PAE of the proposed PA is enhanced by 4.8% which is achieved by the excellent performance of the proposed HCC.

V. CONCLUSION

In this article a high-efficiency inverse class-F PA has been implemented by a novel 3/4 spiral DGS HCC. We have analyzed the transfer characteristics of the DGS with different dimensions. Compared to conventional DGSs, the 3/4 spiral DGS has a simple structure and its resonance frequencies is convenient to adjust. Using the 3/4 spiral DGS a high-performance HCC has been designed for implementing an inverse class-F PA. Compared to the conventional microstrip

https://doi.org/10.1017/S1759078711000663 Published online by Cambridge University Press

HCC, the proposed HCC has improved harmonics controlling performance with simplified structure and reduced size. The 3/4 spiral DGS HCC can be modeled by three parallel RLC resonators and the parameters of the equivalent circuit have been calculated. Moreover, two inverse class-F PAs have been implemented for validation. Due to the simplified structure of the 3/4 spiral DGS HCC, the size of the proposed amplifier decreases by 20%. The experimental results show that the gain and the PAE of the proposed inverse class-F power are enhanced by 1.5 dB and 4.8%, respectively. With excellent performance and reduced size the proposed PA can be of wide application.

REFERENCES

[1] Ma, L.; Jia, D.: The competition and cooperation of WiMax, WLAN and 3G, Mobile Technology, in Applications and Systems 2nd Int. Conf., November 2005, 1–5.

[2] Raab, F.H.: Class-E, class-C, and class-F power amplifiers based upon a finite number of harmonics. IEEE Trans. Microw. Theory Tech., **49** (8) (2001), 1462–1468.

[3] Cripps, S.C.: RF Power Amplifiers for Wireless Communications, Artech House, Norwood, MA, 1999.

[4] Gao, S.: High efficiency class-F RF/microwave power amplifiers. IEEE Microw. Mag., **7** (1) (2006), 40–48.

[5] Raab, F.H.: Class-F power amplifiers with maximally flat waveforms. IEEE Trans. Microw. Theory Tech., **45** (11) (1997), 2007–2012.

[6] Woo, Y.Y.; Yang, Y; Kim, B.: Analysis and experiments for high-efficiency class-F and inverse class-F power amplifiers. IEEE Trans. Microw. Theory Tech., **54** (2006), 1969–1974.

[7] Sheikh, A.; Roff, C.; Benedikt, J.; Paul J. Tasker: Peak class F and inverse class F drain efficiencies using Si LDMOS in a limited bandwidth design. IEEE Microw. Wirel. Compon. Lett., **19** (7) (2009), 473–475.

[8] Ahn, D.; Park, J.S.; Kim, C.S.; Kun, J.; Qian, Y.; Itoh, T.: A design of the lowpass filter using the novel microstrip defected ground structure. IEEE Trans. Microw. Theory Tech., **49** (1) (2001), 86–93.

[9] Kim, C.S.; Park, J.S.; Ahn, D.; Lim, J.B.: A novel 1-D periodic defected ground structure for planar circuits. IEEE Microw. Guid. Wave Lett., **10** (4) (2000), 131–133.

[10] Lim, J.S.; Kim, H.S.; Park, J.S.; Ahn, D.; Nam, S.: A power amplifier with efficiency improved using defected ground structure. IEEE Microw. Wirel. Compon. Lett., **11** (4) (2001), 170–172.

[11] Lim, J.S.; Lee, S.W.; Kim, C.S.; Park, J.S.; Ahn, D.; Nam, S.: A 4:1 unequal Wilkinson power divider. IEEE Microw. Wirel. Compon. Lett., **11** (2001), 124–126.

[12] Choi, H.J.; Lim, J.S.; Jeong, Y.C.: A new design of Doherty amplifier using defected ground structure. IEEE Microw. Wirel. Compon. Lett., **16** (12) (2006), 687–690.

[13] Choi, H.; Shim, S.; Jeong, Y.; Lim, J.; Kim, C. D.: A compact DGS load-network for highly efficient class-E power amplifier, in Microwave Conf., 2009. EuMC 2009. European, 2009, 492–495.

[14] Kim, C.S.; Lim, J.S.; Kang, K.Y.; Park, J.I.; Kim, G.Y.; Ahn, D.: The equivalent circuit modeling of defected ground structure with spiral shape. IEEE MTT-S Int. Microw. Symp. Dig., **3** (2002), 2125–2128.

[15] Jeong, Y.C.; Jeong, S.G.; Lim, J.S.; Nam, S.: A new method to suppress harmonics using $\lambda/4$ bias line combined by defected ground structure in power amplifiers. IEEE Microw. Wirel. Compon. Lett., **13** (12) (2003), 538–540.

[16] Ynag, G.M.; Jin, R.; Vittoria, C.; Harris, V.G.; Sun, N.X.: Small ultra-wideband (UWB) bandpass filter with notched band. IEEE Microw. Wirel. Compon. Lett., **18** (3) (2008), 176–179.

[17] Woo, D.-J.; Lee, T.-K.: Suppression of harmonics in Wilkinson power divider using dual-band rejection by asymmetric DGS. IEEE Transactions Microwave Theory and Techniques, **53** (2005), 2139–2144.

[18] Lim, I.S.; Lee, B.S.: Design of defected ground structures for harmonics control for active microstrip antenna, in Proc. IEEE AP-S Int. Symp., vol. 2, 2002, 852–855.

[19] White, P.: Effect of input harmonic terminations on high efficiency class B and class F operation of PHEMT devices. IEEE MTT-S Int. Symp. Dig., **3** (1998), 1611–1614.

Shilei Jin received the B.S. degree in Electronic Information Science and Technology fromJiangSu University of Science and Technology, China, in 2005 and M.S. degree in Radio Engineering from Southeast University, China, in 2008. He is currently working toward the Ph.D. degree in State key lab of Millimeter Waves, Southeast University.His current research interests include high efficient and linear RF power amplifiers and multimode & multiband wireless access communications.

Jianyi Zhou received the B.S.E.E., M.S.E.E., and Ph.D. degrees from Southeast University, Nanjing,China, in 1993, 1996, and 2001, respectively. In 1996, he joined the faculty of the Department of Radio Engineering, Southeast University, as an Assistant Professor, and became a Lecturer in 1998, an Associate Professor in 2001, and a Professor in 2005. His researches focus on RF circuits and systems in mobile communications.

Lei Zhang received the M.S. and Ph.D. degrees in radio engineering from Southeast University, Nanjing, China, in 1999 and 2010 respectively. He is currently with the School of Information Science and Engineering, Southeast University. His current research includes RF/microwave PA design and linearization techniques.

https://doi.org/10.1017/S1759078711000663 Published online by Cambridge University Press